

BUDA: Boundless Unsupervised Domain Adaptation in Semantic Segmentation

Maxime Bucher¹, Tuan-Hung Vu¹, Matthieu Cord^{1,2}, and Patrick Pérez¹

¹ valeo.ai, France

² Sorbonne Université, France

`firstname.lastname@vimeo.com`

Abstract. In this work, we define and address “Boundless Unsupervised Domain Adaptation” (BUDA), a novel problem in semantic segmentation. BUDA set-up pictures a realistic scenario where unsupervised target domain not only exhibits a data distribution shift w.r.t. supervised source domain but also includes classes that are absent from the latter. Different to “open-set” [27] and “universal domain adaptation” [41], which both regard never-seen objects as “unknown”, BUDA aims at explicit test-time prediction for these never-seen classes. To reach this goal, we propose a novel framework leveraging domain adaptation and zero-shot learning techniques to enable “boundless” adaptation on the target domain. Performance is further improved using self-training on target pseudo-labels. For validation, we consider different domain adaptation set-ups, namely synthetic-2-real, country-2-country and dataset-2-dataset. Our framework outperforms the baselines by significant margins, setting competitive standards on all benchmarks for the new task.

Code and models are available at: <https://github.com/valeoai/buda>.

Keywords: domain adaptation, zero-shot learning, semantic segmentation

1 Introduction

Detailed interpretation of operating environments is crucial for autonomous systems like self-driving cars. Aiming at such an exhaustive scene understanding, most recent vision systems conduct semantic segmentation, the task of predicting semantic classes for all scene pixels. Similar to other perception modules, significant shifts in train (source domain) and test (target domain) distributions drastically degrade the segmentation performance. Many works [16, 35, 37], proposed unsupervised domain adaptation (UDA) techniques to address such *domain gaps* while alleviating the taxing need for label collection on target domain. Recent works introduced relaxed domain adaptation (DA) set-ups in which source and target label-sets differ. For example, partial DA [6, 42] is the case where source label-set contains the target one. Differently, open-set DA [27] assumes that each domain holds a private set of classes while sharing some other ones in common. More challenging, universal DA [41] allows having a completely

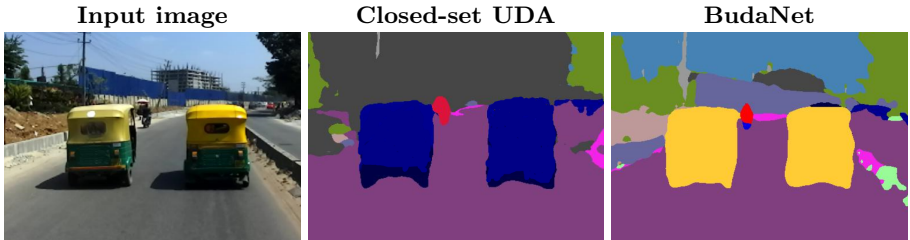


Fig. 1: **Illustration of BudaNet, the proposed approach to the new problem of Boundless Unsupervised Domain Adaptation.** At test time, for an input image (left), we display the closed-set UDA segmentation result (middle) as well as BudaNet segmentation result (right). Both “**tuk-tuk**” vehicles corresponding to unseen classes only appearing in the target domain have been correctly identified by our model. Our approach is able to deal with new classes for which no images have been provided during training. The model trained following the closed-set UDA setting wrongly predicts these new vehicles as a mix of **car** and **truck**.

unknown target label-set. These preceding efforts all contribute to move toward more practical domain adaptation.

In open-set and universal DA settings, new objects from unseen classes in target domain are all classified as “unknown”. Nevertheless, for real-life scenarios where target label-set is indeed *boundless*, one could expect the final system to predict unseen classes explicitly. For example, one might require that the perception model, once trained using European driving scenes (with seen vehicle classes), behaves well on Indian streets with new kinds of vehicles like “tuk-tuk” (unseen class). This task is not covered by above mentioned forms of DA. We call it “Boundless Unsupervised Domain Adaptation”, or BUDA in short, and we propose ways to attack it in the present work.

In particular, we introduce a full semantic segmentation pipeline, BudaNet, that jointly addresses two main challenges: (1) Bridging the domain gap between source and target; (2) Learning discriminant visual representations for never-seen objects in the target domain. In a standard segmentation framework, we propose an UDA strategy to mitigate the distribution gap of source-target seen classes without causing unwanted misalignment to unseen ones. We then introduce a novel deep domain-aware model to generate, from all classes, visual features for both domains. By using this generative model, we collect target’s unseen features, coupled with seen ones from source, to learn the last classification layer of BudaNet. Last, we refine BudaNet with a step of self-training using pseudo-labels on the target domain. The resulting behavior of our system is illustrated in Figure 1.

In summary, our contribution is three-fold:

- We introduce a new task named Boundless Unsupervised Domain Adaptation. The problem is both challenging and meaningful for real-life applications.
- We propose BudaNet, a novel architecture and associated learning scheme, which bridges source-target domain discrepancy while learning how to map never-seen target class labels to relevant visual representations.

- We propose various BUDA set-ups with different kinds of domain gaps, i.e. synthetic-2-real, country-2-country and dataset-2-dataset. BudaNet demonstrates promising results and significantly outperforms the baselines. With this new form of DA task and the proposed BudaNet approach to solve it, we advocate for more practical and ubiquitous domain adaptation in which target label-set is boundless.

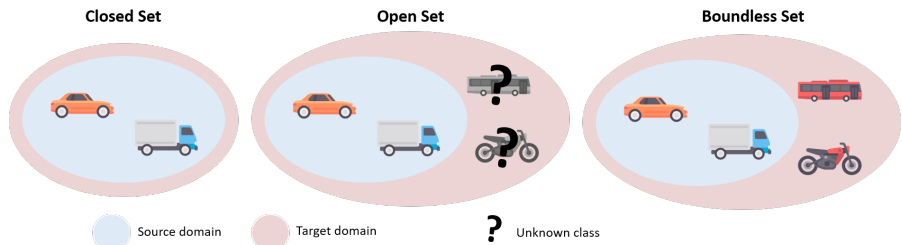


Fig. 2: **Different UDA settings.** In contrast with classic UDA (‘closed set’ hypothesis), boundless UDA (BUDA) assumes that source and target label-sets differ. In addition, unlike the ‘open-set’ setting where objects from private target classes are classified in a single “Unknown” category, BUDA allows the target classes to be explicitly predicted.

2 Boundless UDA related work

In this section, we briefly go through previous UDA works, and position our setting with respect to them. We also review some zero-shot learning techniques that play an important role in the proposed framework.

Unsupervised domain adaptation. Most existing UDA works consider the classic setting in which source and target label-sets are the same. Though approaching UDA via different angles, these works are in the same vein of learning task-dependent domain-invariant features, i.e. minimizing inter-domain discrepancy of feature distributions. Popular techniques include regularizing the maximum mean discrepancy [24], matching deep activation correlation [34], aligning source-target distributions via adversarial training [13, 16], self-training [22, 40, 45] or self-ensembling [11, 44]. Recently, UDA for complex recognition tasks like detection [8] and semantic segmentation [17] have received more attention. Such tasks often require special techniques to handle as well spatial layout [35, 37] or class-proportion [45]. While the standard UDA setting facilitates investigations and helps gain fundamental insights, it is still far from the real-life scenarios.

Some recent works propose techniques in more relaxed UDA settings. In those cases, differences between source and target label-sets make direct distribution alignment approaches less effective. For partial DA, Cao *et al.* align class-wise distributions using multiple domain discriminators [6], while Zhang *et al.* adopt an auxiliary domain classifier to estimate source sample importance [42]. In open-set DA, where source and target can hold private label-sets, a common practice is to use an “unknown” class gathering all target’s private objects [27, 31]. In [41],

the authors introduce a more extreme setting of universal DA, which imposes no prior knowledge on the target label-set.

In the present paper, we consider yet another extension of the classical UDA setting to deal with complex but realistic situations. In this setting, the system is expected to handle explicitly new objects from unseen classes at test time, which means in the target domain. Here, the target label-set is thus unbounded and we coin this novel task boundless UDA (BUDA). In Figure 2, we illustrate BUDA alongside other UDA settings. Opposite to the open-set setting in [31], the source label-set in BUDA is a subset of target label-set. BUDA is different to both open-set and universal DA, because it explicitly asks for all prediction labels at test time. Also worth noting is that our work tackles the complex task of semantic segmentation, where works on open-set and universal UDA concern only classification.

Aiming for a more practical DA, we argue that, given minimal semantic prior, the final system should be capable of explicitly predicting unseen classes. In search of such minimal and practically accessible prior, we opted for the target label-set. More specifically, all target *class names* are assumed to be known before-hand, certainly something effortless to achieve.

Dealing with unseen classes. Zero-Shot Learning (ZSL) aims to recognize unseen classes based on their semantic associations with seen classes. To this end, attributes [21], description [28] or even word embedding [12] have been shown to be effective, shared semantic representations that allow transferring knowledge from seen to unseen classes. In this work we use word2vec [26] as it is extracted at minimal cost and alleviates the need to define and assign hundreds of attributes.

ZSL for image classification has been actively studied in the literature [1, 3, 4, 14, 20, 29, 32, 39, 43] and existing methods can be generally categorized into the following two groups. The first group [1, 3, 20, 29, 32, 43] addresses ZSL as an embedding problem and maps image data and class descriptions into a common space where semantic similarity translates into spacial proximity. The second group [4, 14, 39] of methods learns from visual and semantic features of seen classes and produces generators that can synthesize visual features based on class semantic descriptions. The synthetic features are then used to train a standard classifier for object recognition. This second type of methods has been shown to be more effective than embedding approaches as it reduces the inherent bias toward seen classes. In this work we leverage this type of generative techniques.

Very recently zero-shot learning has been extended to semantic segmentation [5, 18, 38]. [5] introduces the task by combining a deep visual segmentation model with an approach to generate visual representations from semantic word embeddings. [18] proposes variational mapping of the class label embedding vectors to the visual space. [38] introduces a model with a visual-semantic embedding module to encode images in the word embedding space and a semantic projection layer that produces class probabilities.

The present work is inspired by zero-shot learning as we propose to generate image features for the target label-set from semantic representation. However, our BUDA framework differs from classic ZSL in two ways. Firstly, training images

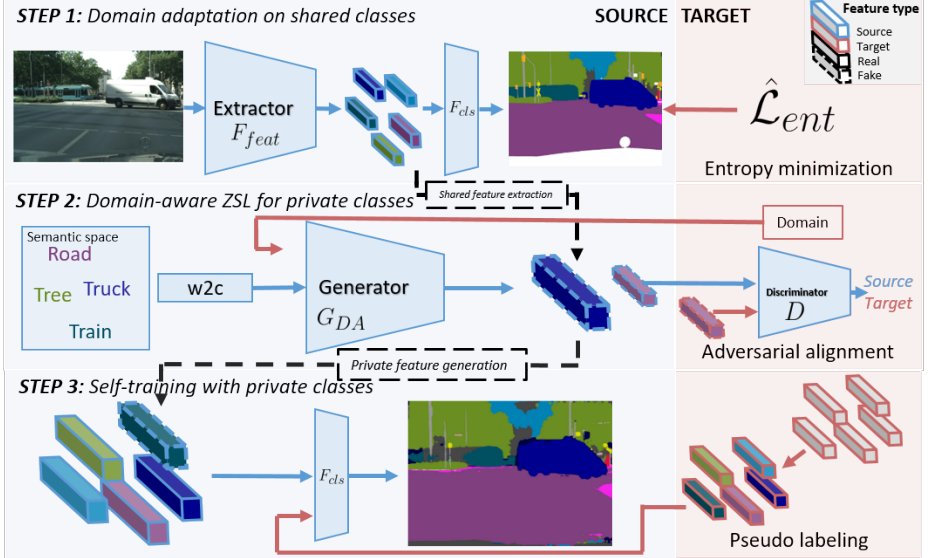


Fig. 3: **BudaNet architecture and learning framework.** Our BudaNet learning strategy consists of three steps: Train the semantic segmentation network with domain alignment only for shared classes; Extract image features and use them as supervision for domain-aware generative model training; Combine the generated features with real ones for classification layer fine-tuning. The red-background pane (right) corresponds to the three proposed strategies for domain alignment, zero-shot learning on target domain and self-training with private classes. Black-dash arrows indicate connections between the steps. Colored arrows distinguish source *vs.* target flows.

with unseen classes are available but are unlabeled, whereas they would not be available at all during training in a pure ZSL setting. Secondly, test images stem from a domain that differs from labeled training domain, opening the door to the domain shift problem.

3 Proposed framework: BudaNet

We first formulate the new task of Boundless Unsupervised Domain Adaptation (BUDA). A training set $\mathcal{D}^s = \{(\mathbf{x}_i^s, \mathbf{y}_i^s)\}$ is available in the source domain, composed of color images $\mathbf{x}_i^s \in \mathbb{R}^{H \times W \times 3}$ of size $H \times W$, and the associated C_s -class ground-truth segmentation maps $\mathbf{y}_i^s \in (1, C_s)^{H \times W}$. A set $\mathcal{D}^t = \{\mathbf{x}_i^t\}$ of unlabelled color images from the target domain is also available at train time.

In BUDA, source's private label-set is empty, all the C_s classes are shared with the target domain classes. However, target domain holds a private label-set of C_p classes. Effectively, at run-time, we want to classify each target pixel as one of the $C_s + C_p$ classes. From now on, to simplify notations, we interchangeably write C_s and C_p as the shared/private label-sets or their corresponding sizes.

In BUDA, we know before-hand all the $C_s + C_p$ class labels. In order to exploit the semantic relations between the classes of interest, we adopt the ‘word2vec’ model [26] learned on a dump of the Wikipedia corpus.

A natural approach for BUDA is to join zero-shot learning (to handle private classes) and domain adaptation (to mitigate domain-shifts) techniques. However, the presence of private classes only in one domain asks for careful consideration from both adaptation and zero-shot perspectives. Indeed, as the final objective is to discriminate both shared and private classes, a direct distribution alignment across domains should be avoided to not mix-up undesirably features of shared and private classes. Regarding zero-shot techniques, their trivial adoption fails to address the mismatch between source and target visual feature distributions, which eventually results in off-track mappings to private target features. These two points are discussed in Sections 3.2 and 3.3.

In this work, we propose a multi-step framework, coined as BudaNet, with dedicated strategies to address the aforementioned concerns. Section 3.1 overviews the base zero-shot pipeline which helps to handle never-seen classes in semantic segmentation. Section 3.2 introduces our UDA strategy to align shared classes across domains with minimal negative alignment effects on private features. In Section 3.3, we present the novel domain-aware generative model to generate synthetic private target features. Lastly, Section 3.4 details the final self-training procedure for the classifier.

3.1 Base zero-shot pipeline

We now revisit a pure non-adaptation zero-shot semantic segmentation (ZS3) pipeline [5] trained only on source images. This pipeline is built on top of an existing semantic segmentation network F , i.e. DeepLabv3+ [7]. To facilitate explanations, we decouple F into two consecutive parts: F_{feat} as the feature extractor and F_{cls} as the final 1×1 convolutional classification layer.

The base zero-shot pipeline consists of three steps:

1. Training a segmentation network F using source supervision on shared classes. Once trained, the feature extractor F_{feat} can compute visual features of C_s shared classes using source images.
2. Training a generative network G conditioned on shared class embeddings to generate corresponding visual features. Ground-truths are shared features extracted from Step 1. The high-level idea is that geometric relations among classes in the embedding space are transferred to the generated feature space, which helps G to handle the C_p private classes.
3. Training the last classification layer F_{cls} of F with private features (generated by G after Step 2) and shared features (computed in Step 1).

The final model is composed of F_{feat} from Step 1 and F_{cls} from Step 3. In detail, the segmentation network F and the classifier F_{cls} are trained using standard segmentation cross-entropy loss \mathcal{L}_{seg} . We follow [5] and adopt a generative moment matching network (GMMN) as G , trained with maximum mean discrepancy loss \mathcal{L}_{GMMN} . Figure 3, to the left, illustrates the pipeline. Our proposed BudaNet is built upon such a base three-steps paradigm.

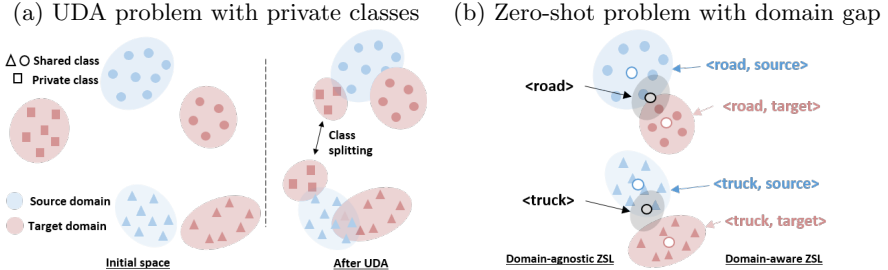


Fig. 4: **BUDA challenges.** (a) Existing UDA techniques, ignoring the presence of target private classes, tend to shift target features to shared-class clusters. (b) With the presence of domain gap, learning domain-agnostic mappings (black arrows) from word embedding space to visual space is sub-optimal as only mean modes (black circles) are captured. Instead, our domain-aware generative model can map to domain-specific modes (blue or red circles).

3.2 BudaNet Step 1: Domain adaptation on shared classes

A pure zero-shot model is only capable of handling shared and private classes at test time, yet fails to address the domain gap. One straight-forward solution for BUDA is to use UDA techniques while training F in Step 1, with the hope that F_{feat} can extract domain-invariant features. Additional unlabeled target images are used for this purpose.

We study two recent UDA techniques in segmentation, MinEnt (self-training) and AdvEnt (adversarial training), both introduced in [37]. With MinEnt, the unsupervised entropy loss \mathcal{L}_{ent} , applied on target samples, is jointly optimized with the supervised segmentation loss \mathcal{L}_{seg} on source samples. \mathcal{L}_{ent} is the sum of pixel-wise target prediction entropies. Differently, AdvEnt approaches global distribution alignment via adversarial training on the weighted self-information space. We refer readers to the original work in [37] for more details.

As mentioned earlier, the source-target label-set mismatch prevents direct alignment between source and target visual distributions. Figure 4-(a) illustrates the problem caused by brute-force adoption of existing UDA techniques in the presence of private classes. Indeed by design, AdvEnt, using global output-space alignment, and MinEnt, using global entropy aggregation, do not differentiate between shared and private classes, which eventually results in undesirable “clusters” of mixed shared and private features.

We propose a simple yet effective strategy based on MinEnt to mitigate the above concern. A segmentation network F^{pre} is first pre-trained only on C_s shared classes of source domain. We then use F^{pre} to produce shared-class predictions on the target training images, which may include both shared and private objects. We argue that, as F^{pre} has never observed private classes at the pre-training phase, top-confident predictions coming from F^{pre} should mostly constitute of shared-class pixels. Effectively, applying entropy minimization solely on such top-confident pixels minimizes the risk of misalignment in the presence of private target features. We then fine-tune F , initialized with F^{pre} , using the optimization objective $\min_{\theta_F} \frac{1}{|\mathcal{D}^s|} \sum_{\mathbf{x}^s} \mathcal{L}_{seg}(\mathbf{x}^s, \mathbf{y}^s) + \frac{\lambda_{ent}}{|\mathcal{D}^t|} \sum_{\mathbf{x}^t} \hat{\mathcal{L}}_{ent}(\mathbf{x}^t)$, where λ_{ent} controls

the weight of entropy term $\hat{\mathcal{L}}_{ent}$. Different to \mathcal{L}_{ent} , to compute $\hat{\mathcal{L}}_{ent}$, we only sum prediction entropies of pixels in the top $k\%$ most-confident set pre-determined by F^{pre} . Figure 3 visualizes the Step 1 operating on both source and target.

3.3 BudaNet Step 2: Domain-aware ZSL for private classes

Part of domain shifts come from the difference in nature between domains, and should always be present no matter the classes, whether shared or private. Although for BUDA we assume the absence of private classes in source domain, if there still appeared a private instance in source, its appearance should be non-negligibly different from corresponding ones in target. For example, similar to “cars”, “tuk-tuks” images if taken in Paris should look different from ones taken in India, due to distinct weather and illumination of each city. We thus find it crucial to take domain information into account in Step 2 where the goal is to synthesize private target features. One may argue that after Step 1, the two domains are already aligned and the domain-invariant feature extractor F_{feat} should be ready as is for feature synthesis. However, no existing UDA technique guarantees perfect and universal alignment across domains, which we thus do not expect either in our approach.

We propose a novel domain-aware generative model, learning to synthesize visual features for both source and target domains. The generative model G is modified such that it is conditioned not only on class embedding but also on domain (source or target). Now the modified model can output shared features for both source and target. We note that, although our objective is to generate domain-aware features, those stemming from the same classes should be rather close. Intuitively, we want our generator to mimic well the feature generator F_{feat} , which produces close source and target feature distributions (as being the effect of the adaptation Step 1) yet still exhibiting certain discrepancies (as discussed above). To this end, we leverage adversarial training. In details, we introduce an additional discriminator D trying to distinguish source-target generated features. At train time, D minimizes the binary cross-entropy classification loss; meanwhile, the generative model trained with an additional adversarial loss \mathcal{L}_{adv} tries to confuse D . Training is now based on the two losses: \mathcal{L}_{GMMN} as in Section 3.1 and the adversarial loss \mathcal{L}_{adv} . Loss details are given in Appendix A.

Generative training is supervised by real shared features coming from both source and target. While on source we can easily assign class labels to shared features using ground-truth maps, on target we must opt for a heuristic pseudo-labeling strategy. Specifically, we evaluate F (pre-trained in Step 1) on the target training set. For each pixel, we assign the class with highest prediction probability as its pseudo-label. Here pseudo-labeling has two major limitations: no correctness guarantee and private pixels in target images are assigned as C_s shared labels. To mitigate such negative effects, only the top $p\%$ of the most confident pseudo-labels are kept; the rest are ignored during training. Doing that, we improve pseudo-label quality for shared classes, and also minimize the number of private pixels in the kept set. In Figure 3, the strategy is illustrated as Step 2.

The domain-aware generative model is coined as G_{DA} . In Figure 4-(b), we illustrate different outcomes of our proposed model as opposed to one without domain-awareness. As G_{DA} can capture domain-specific modes on the visual feature space, we expect better generalization to private classes on target domain.

3.4 BudaNet Step 3: Self-training with private classes

We start by only pre-training the final classification layer F_{cls} with shared source features used in Step 2 and the generated private features coming from G_{DA} – see Figure 5 (left). Once F_{cls} is trained, the network can now handle both shared and private objects at once, which effectively can be used to extract pseudo-labels on target training set. The whole segmentation network F is then fine-tuned again with pseudo-labels – similar to above, we only train on top confident ones. Differently to previous steps, pseudo-labels now cover both C_s shared and C_p private classes. Figure 5 and Figure 3-(Step 3) illustrate the presented self-training strategy. In Figure 5-(right) the decision boundaries, learned after pre-training F_{cls} (blue lines) are shifted to new positions better adapted for target domain after fine-tuning F (black lines).

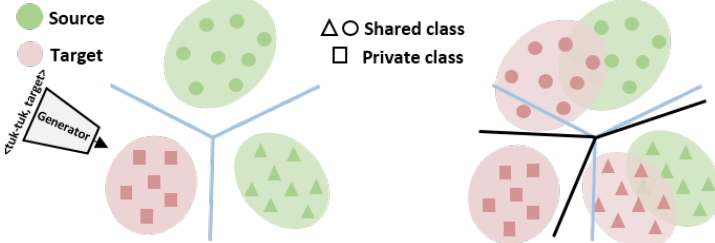


Fig. 5: **Self-training with private classes.** (Left) Pre-training F_{cls} using aligned source features of shared classes used in Step 2 and features generated for private classes, e.g., “tuk-tuk” indicated with squares. Solid lines illustrate the decision boundaries. (Right) Fine-tuning the whole segmenter F using only pseudo-labeled target features – green points are there to contrast with the left figure but not used to train F .

4 Experiments

In Section 4.1, we introduce our set-ups as well as some implementation details. Section 4.2 presents the main results followed by ablation studies in Section 4.3.

4.1 Experimental details

BUDA scenarios. To evaluate our approach, we define three BUDA scenarios: *synthetic-2-real*, *country-2-country* and *dataset-2-dataset*. These very different set-ups allow investigating adaptation from multiple angles of practical interest.

In the *synthetic-2-real* set-up, available at train time are labelled synthetic data and unlabeled real images. The zero-cost (and zero-risk) source label acquisition

makes this configuration especially appealing for semantic segmentation task. We use SYNTHIA-RAND-CITYSCAPES split of SYNTHIA dataset [30] containing 9,400 synthesized images as for source domain. The target domain images are from Cityscapes dataset [9] with 2,975 images for training and 500 images for test. In this set-up, we consider 16 shared classes, previously used in some closed-set UDA works [16, 35, 37]. Differently, our target domain holds a private label-set of 3 classes: “terrain”, “truck” and “train”.

The *country-2-country* set-up addresses the very practical use-case where a model trained using data from one region is deployed in other parts of the world. In details, source domain is the Cityscapes dataset acquired from 50 cities in Germany; while for target domain, we use images from the India driving dataset (IDD) [36]. There is indeed a large gap on vehicles as well as on urban layout between Germany and India. While common vehicles like cars, trucks or buses exist almost everywhere in the two countries, only in India we observe auto-rickshaws. It is also worth mentioning that class distributions are very different, i.e. in India streets, the most frequent vehicle is motorbike while in Germany, car is more prevalent. Such unique signatures of different countries are though interesting yet challenging for applications like self-driving cars. More into details, we use for training 2,975 real Cityscapes images with annotations along with 6,993 unlabeled IDD images. There are 19 shared classes between the two datasets and 2 private classes only in IDD: “auto-rickshaw” (a.k.a. “tuk-tuk”) and “animal”. We evaluate models on 981 IDD images for the total 21 classes.

Our last BUDA set-up is *dataset-2-dataset*: Pascal-VOC [10] and MS-COCO [23] as source and target domains. As both were collected from the Internet, one may expect that the two datasets are very similar. The big difference lies in the scene complexity and level of annotation done in each: while Pascal-VOC images mostly have a single centered object with a limited 20-class label-set, MS-COCO images are more complex with multiple objects exhaustively annotated. Still, as the visual gap is small between the two datasets, we do not expect very significant performance drop in the shared classes. The challenge clearly appears once we consider target’s private label-set. In detail, there are 1,464 VOC images and 118k COCO images used in training. We consider, in the main experiment, 20 shared classes and 5 target private classes: “truck”, “bench”, “zebra”, “giraffe” and “laptop”. For validation, we use 5000 COCO images which contain at least one of the 25 classes.

In BUDA, private classes *must not* appear in the source domain. This constraint leaves us 2-3 private classes in the two first scenarios. Since this limitation does not apply to *dataset-2-dataset*, we could conduct an ablation study on this scenario in Section 4.3 with more private classes, i.e. up to 20.

Model implementation. We adopt the DeepLabv3+ framework [7] built upon the ResNet-101 [15] base deep CNN architecture. The SGD [2] optimizer is used with polynomial learning rate decay with the base learning rate of $10e^{-2}$, weight decay $1e^{-4}$ and momentum 0.9.

Generative models G and G_{DA} are multi-layer perceptrons having a single hidden layer with leaky-ReLU non-linearity [25] and dropout [33]. We fix the

Table 1: Semantic segmentation performance in the three setups.

(a) SYNTHIA → Cityscapes										
Model	Shared			Private			Overall			
	PA	MA	mIoU	PA	MA	mIoU	hPA	hMA	hIoU	
Supervised	95.1	68.1	61.7	58.1	60.0	48.2	72.1	63.8	54.1	
Oracle	94.3	65.7	56.4	50.1	45.9	31.5	65.4	54.0	40.4	
ZS3Net (source only) [5]	80.3	43.1	28.1	9.0	40.7	6.9	16.2	41.9	11.1	
ZS3Net + UDA	85.3	42.4	30.1	12.5	46.8	8.2	21.8	44.9	12.8	
ZS3Net + Adaptation	89.9	42.6	35.0	18.6	51.1	8.9	30.8	46.5	14.2	
BudaNet	93.0	46.0	36.2	26.9	58.7	17.0	41.7	51.6	23.1	
(b) Cityscapes → IDD										
Model	Shared			Private			Overall			
	PA	MA	mIoU	PA	MA	mIoU	hPA	hMA	hIoU	
Supervised	92.8	65.1	56.9	57.3	61.9	48.0	70.9	63.5	52.1	
Oracle	91.7	63.0	53.1	47.2	41.8	28.8	62.3	50.3	37.3	
ZS3Net (source only) [5]	81.0	43.8	29.2	9.3	41.0	7.9	16.7	42.4	12.4	
ZS3Net + UDA	86.8	40.0	32.4	13.8	45.9	8.1	23.8	42.7	13.0	
ZS3Net + Adaptation	88.3	40.5	32.7	15.9	47.0	8.6	26.9	43.5	13.6	
BudaNet	92.0	47.2	37.3	28.6	58.9	18.5	43.6	52.4	24.7	
(c) Pascal-VOC → MS-COCO										
Model	Shared			Private			Overall			
	PA	MA	mIoU	PA	MA	mIoU	hPA	hMA	hIoU	
Supervised	94.8	68.8	70.1	70.5	61.0	64.3	80.9	64.7	67.1	
Oracle	93.8	68.6	68.0	61.6	57.7	39.9	74.4	62.8	50.3	
ZS3Net (source only) [5]	92.0	67.3	63.3	29.9	51.4	17.3	45.1	58.3	27.2	
ZS3Net + UDA	92.3	68.0	63.3	32.3	50.3	19.5	52.0	47.9	29.8	
ZS3Net + Adaptation	92.3	68.2	63.8	36.2	54.1	20.9	52.0	60.3	31.5	
BudaNet	93.1	68.4	65.0	38.5	56.5	23.8	54.5	61.9	34.8	

number of hidden neurons as 256. Both generative models take as input a semantic class embedding and a 300-dim Gaussian noise vector. G_{DA} additionally accepts a 1-dim vector specifying domain (source or target). Regarding the generative loss \mathcal{L}_{GMMN} , we chose kernel bandwidths of $\{2, 5, 10, 20, 40, 60\}$.

For adversarial training of G_{DA} , we introduce an additional binary classification discriminator D : a fully connected layer takes 256-dim feature vectors and predicts corresponding domains. All generative models are trained using Adam optimizer [19] with a learning rate of $2e^{-4}$.

4.2 Results

Table 1 gathers our results in different setups. Following the generalized zero-shot learning protocol in [5], we consider three common segmentation metrics – pixel accuracy (PA), mean accuracy (MA), mean intersection-over-union (mIoU) – along with their corresponding harmonic means of shared and private results – coined as hPA, hMA and hIOU respectively. The harmonic means are used because the common metrics suffer from the performance bias of shared classes, while our aim is to achieve high accuracy for both shared and private classes.

In each experiment, we report performance for shared, private, and all classes. “Supervised” stands for the model trained with full supervision on target domain. “Oracle” corresponds to the zero-shot framework trained on target data using only

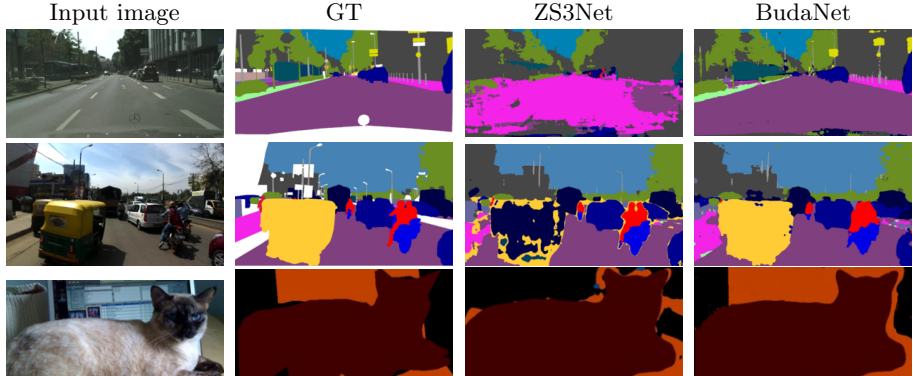


Fig. 6: **Qualitative results of the three set-ups.** The first and second columns show input images and corresponding segmentation ground truth. The third and fourth columns visualize results produced by ZS3Net and BudaNet. From top to bottom: **SYNTHIA**→**Cityscapes** private classes **terrain**, **truck**, **train**; **Cityscapes**→**IDD** private class **tuk-tuk**; and **Pascal-VOC**→**MS-COCO** private class **laptop**. More results are given in Appendix D

shared labels; “ZS3Net (only source)” is a similar network but only trained on source data (based on ZS3Net in [5]). One straight-forward baseline is to directly apply a vanilla UDA technique, i.e. MinEnt [37], in Step 1 without considering the private classes. We name such a baseline as “ZS3Net + UDA”. We note that in the new BUDA setting, existing UDA techniques compare differently, as later reported in Section 4.3; indeed “MinEnt” performs better than a SOTA adversarial training approach. In addition, we consider the proposed strategy introduced in Section 3.2 as a stronger baseline, named as “ZS3Net + Adaptation” in the result tables.

Synthetic-to-Real. Table 1-(a) reports segmentation performance of models trained on SYNTHIA data and evaluated on 19 classes of the Cityscapes validation set. Not surprisingly, the pure zero-shot segmentation model with no adaptation (ZS3Net) produces unfavourable results. The straight-forward baseline (ZS3Net + UDA) does introduce certain improvements over ZS3Net. With shared-class alignment strategy proposed in Section 3.2, our stronger baseline (ZS3Net + Adaptation) performs better on all classes. Finally, BudaNet outperforms all baselines by significant margins for both shared and private classes. Figure 6 (first row) illustrates the merit of our approach. On shared classes, ZS3Net produces noisy segmentation predictions, mistaking “road” pixels with “sidewalk”, while BudaNet produces correct predictions for most pixels. On private classes, i.e. “train” and “truck”, while ZS3Net can only localize small regions, BudaNet provides more complete areas with better contours.

Country-to-Country. Table 1-(b) shows results on 21-class set of the IDD validation set. We observe similar behaviors for the baselines and for BudaNet. While ZS3Net trained only on source domain produces poor results, ZS3Net +

UDA baseline performs better thanks to the straight-forward domain alignment. Using our adaptation strategy in Step 1, the ZS3 + Adaptation baseline enhances recognition performances on all classes. BudaNet introduces gains in both shared and private classes with a significant improvement of +11.1% hIoU in comparison to ZS3 + Adaptation baseline. Figure 6 (second row) visualizes qualitative results. Except that ZS3Net seems to hallucinate “auto rickshaw” category on every vehicles, shared classes predictions of both models look favourable. For private categories, ZS3Net wrongly classifies private “auto rickshaw” pixels with “truck” – a shared class. Qualitatively, our BudaNet results look much better.

Dataset-to-Dataset. Table 1-(c) reports semantic segmentation performances on MS-COCO validation set. We only report results for the 20 shared + 5 private classes and do not consider others. Unlike the two other settings, Pascal-VOC and MS-COCO exhibit a small domain gap since they were both collected from the Internet. Effectively with ZS3Net (no adaptation), the mIoU drop on shared classes is only 4.7% compared to the Oracle. Still, we demonstrate here similar improvements after addressing adaptation and zero-shot challenges. Private classes segmentation results remain much lower due to the absence of training samples for these categories.

Domain alignment with the proposed strategy in Step 1 (ZS3Net + Adaptation) allows improvement on private classes of +3.6% mIoU; shared class scores remain comparable (63.3% vs. 63.8% mIoU). BudaNet helps boost performance in all classes with a hIoU increase of +7.6% in comparison to ZS3Net, most of which accounts to private classes. Figure 6 (last row) reports qualitative examples of ZS3Net and BudaNet. ZS3Net wrongly classifies private object parts as background or shared classes. BudaNet produces more favourable predictions with accurate object contours.

4.3 Ablation studies

Effect of proposed strategies. Table 2 reports 5 ablation experiments, studying the advantages of our proposed strategies. “ZS3Net” is trained only on source (no adaptation). “ZS3Net + UDA” is our baseline with entropy minimization and “BudaNet - Step 1+2+3” is the proposed BUDA network. “MinEnt” stands for entropy minimization while training segmenter F , “Shared only” means applying entropy minimization on top-confident pixels, “Adv. crit” is generator training with adaptation and “Self-training” corresponds to the fine-tuning of the semantic segmentation model. We first observe that brute force entropy minimization contributes to improving performance by 1.7% (“ZS3Net” vs. “ZS3Net + UDA”), which demonstrates the need for domain alignment prior to generative model training. The table indicates that our pseudo-labeled strategy selection for shared pixels in target domain (“ZS3Net + UDA” vs. “BudaNet - Step 1”) significantly increases the performance by 1.4%. For generator training, the combination of source training data with pseudo-labeled target data and the adversarial loss (“BudaNet - Step 1” vs. “BudaNet - Step 1+2”) further improves performance, from 14.2 to 22.0. Finally the proposed “BudaNet - Step 1+2+3” benefits from

Table 2: Ablation experiments on the validation set of Cityscapes.

Setup	MinEnt	Shared only	Adv. crit.	Self-training	hIoU (%)
ZS3Net					11.1
ZS3Net + UDA	✓				12.8
BudaNet - Step 1	✓		✓		14.2
BudaNet - Step 1+2	✓	✓	✓	✓	22.0
BudaNet - Step 1+2+3	✓	✓	✓	✓	23.1

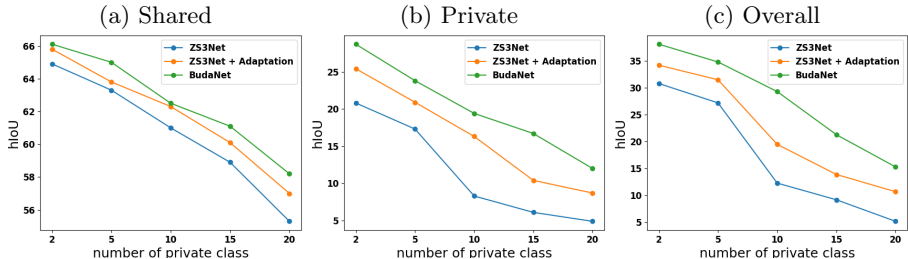


Fig. 7: hIoU (%) results w.r.t. the number of private classes.

self-training (up to 1.1%), at this step the pseudo-labeling strategy makes it possible to exploit the information relating to private features pixels.

Number of private classes. We consider different setups varying in number of private classes in the *dataset-2-dataset scenario*. To this end, we construct the 2-, 5-, 10-, 15- and 20-class private label sets in an incremental manner, meaning that for instance the 10-class private set contains classes in the 5-class set. More details are given in Appendix B. Figure 7 shows curves of hIoU results with respect to the number of private classes. We observe a decreasing trend in performance for all methods when more private classes (respectively fewer shared classes) are used. In all set-ups, the proposed BudaNet (green curves) outperforms the addressed baselines by a significant margin.

Table 3: Adaptation done on shared classes at Step 1.

Model	Cityscapes			IDD			MS-COCO		
	Shar.	Priv.	All	Shar.	Priv.	All	Shar.	Priv.	All
ZS3Net + vanilla AdvEnt	30.1	7.5	12.0	32.3	8.0	12.8	63.4	19.5	29.8
ZS3Net + vanilla MinEnt	30.0	8.2	12.8	32.4	8.1	13.0	63.3	19.5	29.8
ZS3Net + Adaptation*	35.0	8.9	14.2	32.7	8.6	13.6	63.8	20.9	31.5

*: "ZS3Net + Adaptation" is the "BudaNet - Step 1" in Table 2

Domain adaptation strategy on shared classes. In Table 3, we report the negative effects caused by global alignment of existing UDA techniques like vanilla AdvEnt in BUDA. Such a drawback was similarly observed in partial DA and open-set DA works. These experiments echo the arguments developed in Section 3.2 to justify the relevance of the proposed adaptation strategy.

5 Conclusion

In this work we presented BUDA, a novel extension of the classic UDA task, which allows new class predictions at test time. To address this new task, we introduced BudaNet to jointly mitigate domain-gap in the presence of private classes and enable generalization to new object classes in the target domain. BudaNet significantly outperforms several advanced baselines in three challenging settings. We believe that this new task and framework pave the way toward more practical domain adaptation for real-life applications.

A BudaNet loss details

We detail below the different losses introduced in Section 3 of the submission.

- *Cross-entropy segmentation loss.* Given a source sample $(\mathbf{x}^s, \mathbf{y}^s)$ with $\mathbf{P}^{\mathbf{x}^s}$ as the soft-segmentation prediction map, this loss reads:

$$\mathcal{L}_{seg}(\mathbf{x}^s, \mathbf{y}^s) = - \sum_{h=1}^H \sum_{w=1}^W \sum_{c=1}^C \mathbf{y}_{(h,w,c)}^s \log \mathbf{P}_{(h,w,c)}^{\mathbf{x}^s}. \quad (1)$$

For F training in Step 1, we set $C = C_s$. For F_{cls} training in Step 3, we set $C = C_s + C_p$.

- *Entropy loss.* Given a target sample \mathbf{x}^t with predicted soft-segmentation map $\mathbf{P}^{\mathbf{x}^t}$, the entropy loss is:

$$\mathcal{L}_{ent}(\mathbf{x}^t) = \frac{-1}{\log(C_s)} \sum_{h=1}^H \sum_{w=1}^W \sum_{c=1}^{C_s} \mathbf{P}_{(h,w,c)}^{\mathbf{x}^t} \log \mathbf{P}_{(h,w,c)}^{\mathbf{x}^t}. \quad (2)$$

- *Generative loss for G_{DA} .* Given a random sample \mathbf{z} from a fixed multivariate Gaussian distribution, the semantic embedding \mathbf{a} and the domain indicator d (set as 1 for source and 0 for target), new pixel features are generated as $\hat{\mathbf{f}} = G_{DA}(\mathbf{a}, d, \mathbf{z}; \theta_{G_{DA}})$, where $\theta_{G_{DA}}$ are the parameters of G_{DA} . With two random populations $\mathcal{F}(\mathbf{a}, d)$ of real features (from both source and target) and $\hat{\mathcal{F}}(\mathbf{a}, d; \theta_{G_{DA}})$ of generated ones, we have:

$$\begin{aligned} \mathcal{L}_{GMMN}(\mathbf{a}, d) = & \sum_{\mathbf{f}, \mathbf{f}' \in \mathcal{F}(\mathbf{a}, d)} k(\mathbf{f}, \mathbf{f}') + \sum_{\hat{\mathbf{f}}, \hat{\mathbf{f}}' \in \hat{\mathcal{F}}(\mathbf{a}, d; \theta_{G_{DA}})} k(\hat{\mathbf{f}}, \hat{\mathbf{f}}') \\ & - 2 \sum_{\mathbf{f} \in \mathcal{F}(\mathbf{a}, d)} \sum_{\hat{\mathbf{f}} \in \hat{\mathcal{F}}(\mathbf{a}, d; \theta_{G_{adv}})} k(\mathbf{f}, \hat{\mathbf{f}}), \end{aligned} \quad (3)$$

where k is the Gaussian kernel, $k(\mathbf{f}, \mathbf{f}') = \exp(-\frac{1}{2\sigma^2} \|\mathbf{f} - \mathbf{f}'\|^2)$ with bandwidth parameter σ .

- *Discriminator loss.* Given $\hat{\mathbf{f}}^s$ and $\hat{\mathbf{f}}^t$ the two generated features for source (label 1) and target (label 0) domains, this loss reads:

$$\mathcal{L}_D(\hat{\mathbf{f}}^s, \hat{\mathbf{f}}^t) = \mathcal{L}_{BCE}(\hat{\mathbf{f}}^s, 1) + \mathcal{L}_{BCE}(\hat{\mathbf{f}}^t, 0), \quad (4)$$

with \mathcal{L}_{BCE} as the binary cross-entropy loss.

- *Adversarial loss for G_{DA} .* Given $\hat{\mathbf{f}}^t$ the generated feature for target domain, this loss reads:

$$\mathcal{L}_{adv}(\hat{\mathbf{f}}^t) = \mathcal{L}_{BCE}(\hat{\mathbf{f}}^t, 1). \quad (5)$$

To train G_{DA} , we use a weighting factor λ_{adv} for \mathcal{L}_{adv} .

B Number of private classes

In what follows, we detail the private label-sets used in the ablation study where the number of private classes is varied (Section 4.3). As the set of all classes is fixed, shared ones are determined accordingly. The nested sequence of private label-sets is:

- 2 private classes: truck/zebra
- 5 private classes: .../bench/giraffe/laptop
- 10 private classes: .../elephant/umbrella/bear/snowboard/toilet
- 15 private classes: .../laptop/refrigerator/blanket/napkin/stone
- 20 private classes: .../tent/skyscraper/salad/river/pillow

where each label-set with more than 2 classes includes the preceding ones.

C Pseudo-labeling: proportion of retained top-scoring predictions

Table 4: Evolution of the hIoU performance according to the percentage of high-scoring pixels retained for pseudo-labeling. GT: see text for explanations

$p\%$ of high-scoring	10%	30%	50%	70%	100%	GT
Cityscapes hIoU	20.4	21.6	22.0	21.8	17.8	38.9

Effect of the pseudo-labeling percentage in Step 2. Our aim here is to compare different $p\%$ values for the pseudo-labeling strategy on target features. Table 4 shows hIoU results on Cityscapes dataset. Keeping only the highest-scoring predictions, at 10%, results in a drop of performance of 1.6%. One possible explanation is that because the number of training features becomes too low, the model lacks generalization capacity. Conversely, when all predictions are kept ($p = 100\%$), a significant decrease of performance can be observed which confirms the need for an effective pixel selection strategy. Finally, we observe that the performance is better when $p \in [30, 70]$, specifically when $p = 50\%$ with a recognition score of 22.0 hIoU. In the last column of Table 4, “GT”, we report the recognition score when the $p = 50\%$ highest scoring predictions are replaced by their ground truth labels. We observe a performance improvement of 16.9%,

pixel selection technique is therefore an essential element of the method and must be investigated in future work.

In all other steps with pseudo-labeling, we also fix the percentage of retained high scoring predictions as 50%.

D BudaNet qualitative results

Figure 8 shows additional results on Cityscapes. As mentioned in the submission, ZS3Net produces noisy segmentation with, for example, the shared class “person” missing in rows 2 and 3. In the same way, the areas of the private class “truck” are hardly detected and wrongly localized elsewhere in rows 1 and 3. Our BudaNet provides favourable predictions on these areas.

Figure 9 reports additional qualitative results on IDD. Both models produce reasonable segmentation for the shared classes. However, in rows 1 to 4, ZS3Net hallucinates “auto rickshaw” parts on all vehicles. Further, most of “auto rickshaw” pixels are partially predicted or incorrectly classified as “truck” (row 3) or “bus” (row 1, 2 and 3). The last row shows the second private class “animal”. While ZS3Net completely misses the animals on the road, the proposed BudaNet correctly predicts two of them.

In Figure 10, we visualize qualitative results for the other four private classes of MS-COCO dataset. In row 1, while ZS3Net wrongly segments most pixels of the private class “bench” as “chair”, BudaNet can recognize more complete objects. In 2nd and 3rd examples, ZS3Net confuses the private pixels of “giraffe” and “zebra” as “background”. By contrast, BudaNet delivers good predictions for these classes. In the last row, BudaNet is shown to improve performance for the “truck” class.

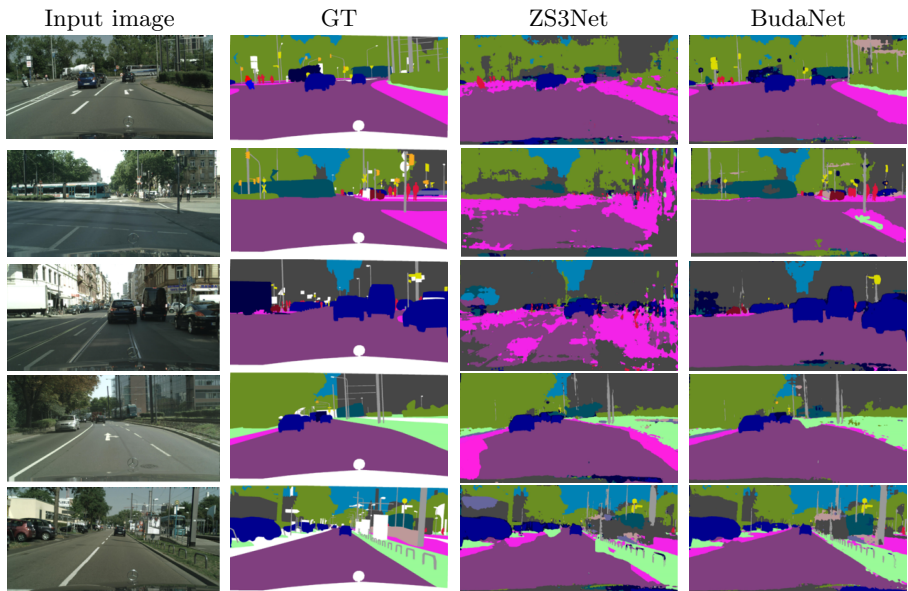


Fig. 8: **Additional qualitative results on Cityscapes.** The left column shows the input image, the second is the ground truth of semantic segmentation. The third shows the segmentation produced by ZS3Net and the last one BudaNet result. Private target classes: `terrain`, `truck`, `train`. Some shared classes: `road`, `side walk`, `car`, `person`, `motorbike`, `tree`, `building`.

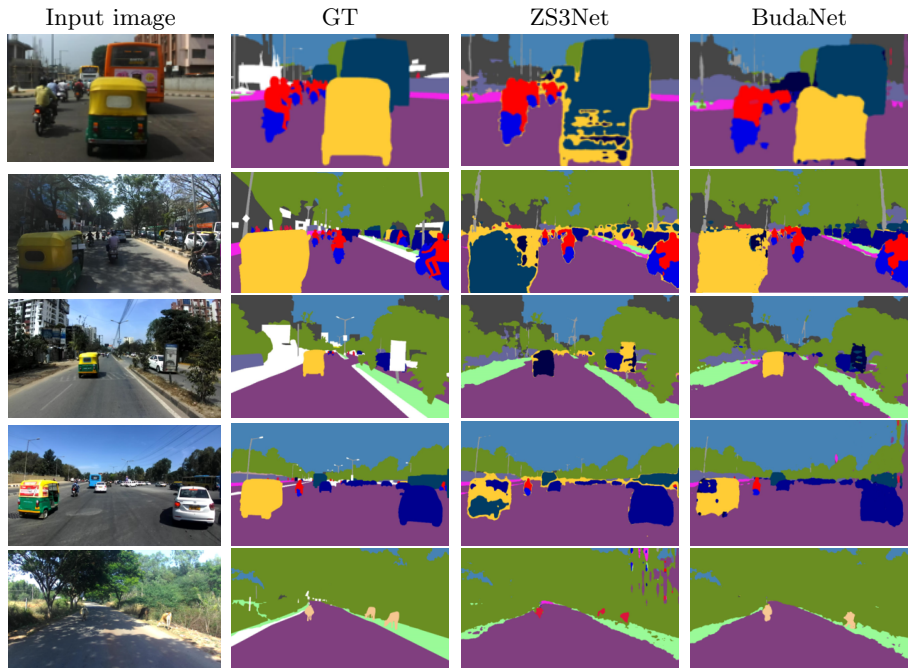


Fig. 9: **Additional qualitative results on IDD.** Similar arrangement as in Figure 8. Private target classes: **tuk-tuk**, **animal**. Some shared classes: **truck**, **road**, **side walk**, **car**, **person**, **motorbike**, **tree**, **building**.



Fig. 10: **Additional qualitative results on MS-COCO.** Similar arrangement as in Figure 8. Private target classes: **bench**, **giraffe**, **zebra**, **truck**. Shared classes: **person**, **cow**, **sheep**, **background**.

References

1. Akata, Z., Reed, S., Walter, D., Lee, H., Schiele, B.: Evaluation of output embeddings for fine-grained image classification. In: CVPR (2015) **4**
2. Bottou, L.: Large-scale machine learning with stochastic gradient descent. In: COMPSTAT (2010) **10**
3. Bucher, M., Herbin, S., Jurie, F.: Improving semantic embedding consistency by metric learning for zero-shot classification. In: ECCV (2016) **4**
4. Bucher, M., Herbin, S., Jurie, F.: Generating visual representations for zero-shot classification. In: ICCV (2017) **4**
5. Bucher, M., Vu, T.H., Cord, M., Pérez, P.: Zero-shot semantic segmentation. In: NeurIPS (2019) **4, 6, 11, 12**
6. Cao, Z., Long, M., Wang, J., Jordan, M.I.: Partial transfer learning with selective adversarial networks. In: CVPR (2018) **1, 3**
7. Chen, L.C., Zhu, Y., Papandreou, G., Schroff, F., Adam, H.: Encoder-decoder with atrous separable convolution for semantic image segmentation. In: ECCV (2018) **6, 10**
8. Chen, Y., Li, W., Sakaridis, C., Dai, D., Van Gool, L.: Domain adaptive faster r-cnn for object detection in the wild. In: CVPR (2018) **3**
9. Cordts, M., Omran, M., Ramos, S., Rehfeld, T., Enzweiler, M., Benenson, R., Franke, U., Roth, S., Schiele, B.: The cityscapes dataset for semantic urban scene understanding. In: CVPR (2016) **10**
10. Everingham, M., Eslami, S.A., Van Gool, L., Williams, C.K., Winn, J., Zisserman, A.: The pascal visual object classes challenge: A retrospective. IJCV (2015) **10**
11. French, G., Mackiewicz, M., Fisher, M.: Self-ensembling for visual domain adaptation. In: ICLR (2018) **3**
12. Frome, A., Corrado, G.S., Shlens, J., Bengio, S., Dean, J., Mikolov, T., et al.: Devise: A deep visual-semantic embedding model. In: NIPS (2013) **4**
13. Ganin, Y., Lempitsky, V.: Unsupervised domain adaptation by backpropagation. In: ICML (2015) **3**
14. Gao, R., Hou, X., Qin, J., Liu, L., Zhu, F., Zhang, Z.: A joint generative model for zero-shot learning. In: Proceedings of the European Conference on Computer Vision (ECCV) (2018) **4**
15. He, K., Zhang, X., Ren, S., Sun, J.: Deep residual learning for image recognition. In: CVPR (2016) **10**
16. Hoffman, J., Tzeng, E., Park, T., Zhu, J.Y., Isola, P., Saenko, K., Efros, A., Darrell, T.: Cycada: Cycle-consistent adversarial domain adaptation. In: ICML (2018) **1, 3, 10**
17. Hoffman, J., Wang, D., Yu, F., Darrell, T.: FCNs in the wild: Pixel-level adversarial and constraint-based adaptation. arXiv:1612.02649 (2016) **3**
18. Kato, N., Yamasaki, T., Aizawa, K.: Zero-shot semantic segmentation via variational mapping. In: ICCV Workshops (2019) **4**
19. Kingma, D.P., Ba, J.: Adam: A method for stochastic optimization. In ICLR (2014) **11**
20. Kodirov, E., Xiang, T., Gong, S.: Semantic autoencoder for zero-shot learning. In: CVPR (2017) **4**
21. Lampert, C.H., Nickisch, H., Harmeling, S.: Attribute-based classification for zero-shot visual object categorization. TPAMI (2013) **4**
22. Li, Y., Yuan, L., Vasconcelos, N.: Bidirectional learning for domain adaptation of semantic segmentation. In: CVPR (2019) **3**

23. Lin, T.Y., Maire, M., Belongie, S., Hays, J., Perona, P., Ramanan, D., Dollár, P., Zitnick, C.L.: Microsoft coco: Common objects in context. In: ECCV (2014) **10**
24. Long, M., Cao, Y., Wang, J., Jordan, M.I.: Learning transferable features with deep adaptation networks. In: ICML (2015) **3**
25. Maas, A.L., Hannun, A.Y., Ng, A.Y.: Rectifier nonlinearities improve neural network acoustic models. In: ICML (2013) **10**
26. Mikolov, T., Sutskever, I., Chen, K., Corrado, G.S., Dean, J.: Distributed representations of words and phrases and their compositionality. In: NIPS (2013) **4**, **6**
27. Panareda Busto, P., Gall, J.: Open set domain adaptation. In: ICCV (2017) **1**, **3**
28. Reed, S., Akata, Z., Lee, H., Schiele, B.: Learning deep representations of fine-grained visual descriptions. In: CVPR (2016) **4**
29. Romera-Paredes, B., Torr, P.: An embarrassingly simple approach to zero-shot learning. In: ICML (2015) **4**
30. Ros, G., Sellart, L., Materzynska, J., Vazquez, D., Lopez, A.M.: The synthia dataset: A large collection of synthetic images for semantic segmentation of urban scenes. In: CVPR (2016) **10**
31. Saito, K., Yamamoto, S., Ushiku, Y., Harada, T.: Open set domain adaptation by backpropagation. In: ECCV (2018) **3**, **4**
32. Socher, R., Ganjoo, M., Manning, C.D., Ng, A.: Zero-shot learning through cross-modal transfer. In: NIPS (2013) **4**
33. Srivastava, N., Hinton, G., Krizhevsky, A., Sutskever, I., Salakhutdinov, R.: Dropout: a simple way to prevent neural networks from overfitting. JMLR (2014) **10**
34. Sun, B., Saenko, K.: Deep coral: Correlation alignment for deep domain adaptation. In: ECCV (2016) **3**
35. Tsai, Y.H., Hung, W.C., Schulter, S., Sohn, K., Yang, M.H., Chandraker, M.: Learning to adapt structured output space for semantic segmentation. In: CVPR (2018) **1**, **3**, **10**
36. Varma, G., Subramanian, A., Namboodiri, A., Chandraker, M., Jawahar, C.: Idd: A dataset for exploring problems of autonomous navigation in unconstrained environments. In: WACV (2019) **10**
37. Vu, T.H., Jain, H., Bucher, M., Cord, M., Pérez, P.: Advent: Adversarial entropy minimization for domain adaptation in semantic segmentation. In: CVPR (2019) **1**, **3**, **7**, **10**, **12**
38. Xian, Y., Choudhury, S., He, Y., Schiele, B., Akata, Z.: Semantic projection network for zero-and few-label semantic segmentation. In: CVPR (2019) **4**
39. Xian, Y., Lorenz, T., Schiele, B., Akata, Z.: Feature generating networks for zero-shot learning. In: CVPR (2018) **4**
40. Xie, S., Zheng, Z., Chen, L., Chen, C.: Learning semantic representations for unsupervised domain adaptation. In: ICML (2018) **3**
41. You, K., Long, M., Cao, Z., Wang, J., Jordan, M.I.: Universal domain adaptation. In: CVPR (2019) **1**, **3**
42. Zhang, J., Ding, Z., Li, W., Ogunbona, P.: Importance weighted adversarial nets for partial domain adaptation. In: CVPR (2018) **1**, **3**
43. Zhang, Z., Saligrama, V.: Zero-shot learning via semantic similarity embedding. In: ICCV (2015) **4**
44. Zhu, X.J.: Semi-supervised learning literature survey. Tech. rep., University of Wisconsin-Madison Department of Computer Sciences (2005) **3**
45. Zou, Y., Yu, Z., Kumar, B., Wang, J.: Domain adaptation for semantic segmentation via class-balanced self-training. In: ECCV (2019) **3**